A Decade of Satellite Ocean Color Observations*

Charles R. McClain

Oceans Branch, NASA Goddard Space Flight Center, Greenbelt, Maryland 20771; email: charles.r.mcclain@nasa.gov

Annu. Rev. Mar. Sci. 2009. 1:19–42

First published online as a Review in Advance on August 21, 2008

The *Annual Review of Marine Science* is online at marine.annualreviews.org

This article's doi: 10.1146/annurev.marine.010908.163650

1941-1405/09/0115-0019$20.00

Key Words

carbon cycle, chlorophyll *a*, marine ecosystems, satellite calibration and validation, SeaWiFS

Abstract

After the successful Coastal Zone Color Scanner (CZCS, 1978–1986) demonstration that quantitative estimations of geophysical variables such as chlorophyll *a* and diffuse attenuation coefficient could be derived from top of the atmosphere radiances, a number of international missions with ocean color capabilities were launched beginning in the late 1990s. Most notable were those with global data acquisition capabilities, i.e., the Ocean Color and Temperature Sensor (OCTS, Japan, 1996–1997), the Sea-viewing Wide Field-of-view Sensor (SeaWiFS, United States, 1997-present), two Moderate Resolution Imaging Spectroradiometers (MODIS, United States, Terra/2000-present and Aqua/2002-present), the Global Imager (GLI, Japan, 2002–2003), and the Medium Resolution Imaging Spectrometer (MERIS, European Space Agency, 2002-present). These missions have provided data of exceptional quality and continuity, allowing for scientific inquiries into a wide variety of marine research topics not possible with the CZCS. This review focuses on the scientific advances made over the past decade using these data sets.

BACKGROUND

Chromophoric dissolved organic matter (CDOM): soluble organic compounds from decayed plant biomass that selectively absorb blue light; also known as gilvin, gelbstoff, and yellow substance

CZCS: Coastal Zone Color Scanner

Atmospheric correction: removal of atmospheric and sea surface signals from the upwelling radiance measured at the top of the atmosphere

OCTS: Ocean Color and Temperature Sensor

MODIS: Moderate Resolution Imaging Spectroradiometer

MERIS: Medium Resolution Imaging Spectrometer

SeaWiFS: Sea-viewing Wide Field-of-view Sensor

The color of the ocean is a very good indicator of the pigment and particulate content of the water. Water and pigments such as chlorophyll *a* and chromophoric dissolved organic matter (CDOM) have well-defined absorption spectra. Water is transparent at blue and green wavelengths, but is strongly absorbing at longer wavelengths. Chlorophyll *a*, the primary photosynthetic pigment found in phytoplankton, has a primary absorption peak near 440 nm. CDOM absorption monotonically increases as wavelength decreases into the ultraviolet (UV). Also, particulate scattering enhances reflectance (ratio of incoming to outgoing light) at longer wavelengths. The net result is a shift from blue water to brownish water as pigment and particulate concentrations increase. The obvious question is whether or not changes in the spectral reflectance are sufficiently correlated with a single pigment such as chlorophyll *a* to be quantitatively useful. If so, the next question is whether or not accurate observations of ocean reflectance could be made from a satellite so that large areas could be surveyed rapidly and routinely.

Using radiometric data from an aircraft, Clarke et al. (1970) published one of the first remote sensing demonstrations of this shift in spectral shape as chlorophyll *a* concentration increased. This group also showed that the atmospheric contribution to the total reflectance increased dramatically with altitude as a result of Rayleigh (gas molecules) and aerosol scattering. In fact, at the top of the atmosphere, the radiance emanating out of the water column contributes no more than 15% of the total radiance. To remove the atmospheric radiance, the correction scheme would need to accurately account for numerous scattering (gases and aerosols), absorption (at least ozone absorption), and surface reflection (sun glint) interactions for a wide range of solar and sensor-viewing geometries. Despite these challenges, NASA approved the Coastal Zone Color Scanner (CZCS) as one of several experimental sensors on the Nimbus-7 mission launched in 1978. The CZCS had ocean color bands at 443, 520, and 550 nm for quantifying changes in the marine spectral slope with pigment concentration. Gordon et al. (1983) published the seminal paper on the atmospheric correction and pigment retrieval methodologies, demonstrating that reasonably accurate pigment concentrations could be derived from a properly designed satellite instrument. A large volume of literature based on the CZCS exists. See Abbott & Chelton (1991), Barale & Schlittenhardt (1993), and the *Journal of Geophysical Research* special issue on ocean color (Mitchell 1994) for extensive reviews.

With the success of the CZCS, a number of missions were approved by various space agencies, some of which were meant for technology development and others for research. The distinction is associated with sensor specifications and performance requirements, coverage, data accessibility, and mission calibration and validation. The Ocean Color and Temperature Sensor (OCTS), Sea-viewing Wide Field-of-view Sensor (SeaWiFS), Moderate Resolution Imaging Spectroradiometer (MODIS), Global Imager (GLI), and Medium Resolution Imaging Spectrometer (MERIS) missions were clearly designed for quantitative global research purposes and incorporated additional wavelengths, on-board calibration capabilities, extended postlaunch validation programs, and routine global coverage. In some cases, e.g., MODIS and MERIS, phytoplankton fluorescence bands were included. Of these sensors, SeaWiFS has provided the longest (more than ten years) data record. The OCTS and GLI data sets are shorter than an annual cycle, although the OCTS was the only sensor to capture the initial phase of the 1997–1998 El Niño–La Niña. MODIS/Terra ocean color data quality issues have limited its use. The MODIS/Aqua data quality is similar to that of SeaWiFS (Franz et al. 2007). The MERIS swath is much narrower than those of SeaWiFS or MODIS, making global coverage less frequent. Consequently, SeaWiFS data have been used in an overwhelming majority of published results to date. This review focuses on results from these recent missions and not on updating the previous CZCS literature reviews. Yoder & Kennelly

(2006) provide a recent overview of satellite ocean color results, many of which are based on the CZCS. The number of refereed journal articles using SeaWiFS data alone is several hundred, so this review provides only a representative sampling across a variety of specific topics.

Vicarious calibration: the adjustment of satellite calibration required to match satellite and inferred top of the atmosphere radiances derived using observed water-leaving radiances

DATA PRODUCTS AND QUALITY

The CZCS global follow-on missions carried high accuracy goals for climate research, which drove the calibration and validation requirements that were based on many lessons learned from the CZCS experience (McClain et al. 2006). These requirements included the need for additional sensor observations in the near-infrared for aerosol corrections, detailed prelaunch sensor characterizations, accurate on-orbit sensor stability monitoring, field observations specifically for postlaunch sensor vicarious calibration, and higher quality in situ radiometry over a more diverse range of ocean provinces. These activities were undertaken by the various space agencies that supported the different ocean color missions; the NASA Sensor Intercomparison and Merger for Biological and Interdisciplinary Oceanic Studies (SIMBIOS) program and the International Ocean Color Coordinating Group (IOCCG) assisted in the coordination between agencies.

On-orbit calibration monitoring is essential for research quality data. SeaWiFS, for example, executed monthly lunar calibration spacecraft maneuvers (Barnes et al. 2004) to image the moon at a constant phase angle (~7°) to monitor stability (**Figure 1**), whereas MODIS incorporated a sophisticated solar diffuser design with a diffuser stability monitor. The Marine Optical Buoy (MOBY) (Clark et al. 1997) was developed and deployed off Lanai, Hawaii just prior to the Sea WiFS launch, providing data for vicarious calibration (Franz et al. 2007) primarily for Sea WiFS and both MODIS sensors. An earlier test deployment covered much of the OCTS period. Similarly, the Bouée pour l'acquisition de Séries Optiques à Long Terme (BOUSOULLE) mooring was deployed in the Mediterranean Sea south of France in support of MERIS (Antoine

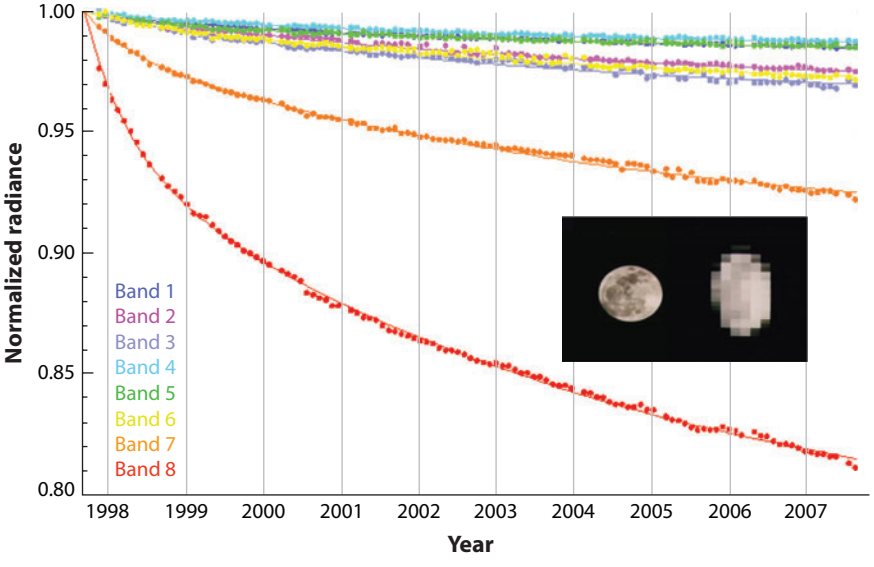

Figure 1

The temporal loss in Sea-viewing Wide Field-of-view Sensor (SeaWiFS) spectral radiometric sensitivity relative to the first lunar calibration. Vertical gray lines denote January 1st of each year. The insert depicts a SeaWiFS image of the moon.

et al. 2008). Field observation improvements required a broad range of activities (Hooker & McClain 2000, McClain et al. 2004a), including the development of measurement protocols (e.g., Hooker & Maritorena 2000; Hooker et al. 2002; Hooker & Morel 2003; Hooker & Zibordi 2005), calibration round-robins (e.g., Meister et al. 2003), pigment analysis round-robins (Claustre et al. 2004), and field instrumentation development, e.g., the SeaWiFS Photometer Revision for Incident Surface Measurements (SeaPRISM) (Zibordi et al. 2004). Time series programs were augmented with optical measurements, e.g., the Hawaii Ocean Time series (HOT), the Bermuda Atlantic Time Series (BATS), the *Acqua Alta* tower (Venice, Italy), the California Cooperative Oceanic Fisheries Investigations (CalCOFI) and the Plumes and Blooms program. Many major cruise programs have emphasized satellite validation data collection, e.g., the Atlantic Meridional Transect (AMT), the Productivité des Systèmes Océaniques Pélagiques, the Benguela Calibration, and the Biogeochemistry and Optics South Pacific Experiment cruises. Data from these and many other sources have been compiled in a quality-controlled database to support science community algorithm development and product validation analyses (Werdell & Bailey 2005).

Water-leaving radiance: the radiance backscattered upward through the air-sea interface

Diffuse attenuation coefficient: the scale length for the exponential decrease of downwelling solar radiation with depth

Fluorescence line height (FLH): the enhancement in water-leaving radiance due to chlorophyll *a* fluorescence above the background radiance

Atmospheric correction algorithms have greatly improved since the CZCS. Gordon & Wang (1994) outlined a strategy for utilizing the SeaWiFS and MODIS near-infrared (NIR) bands to estimate the aerosol radiances in the visible, which has worked quite well except over turbid water and where absorbing aerosols are present. Their approach assumes that ocean reflectance is negligible in the NIR, which allows the atmospheric correction to be decoupled from the ocean subsurface reflectance. A number of turbid water correction schemes have been proposed, e.g., by Siegel et al. (2000) and Lavender et al. (2005). For MODIS, the shortwave-infrared (SWIR) bands can be used for turbid water aerosol corrections because even turbid waters have no significant reflectance at these wavelengths (Wang & Shi 2005), although the MODIS SWIR bands have low signal-to-noise ratio (SNR), which limits their accuracy for this application.

Absorbing aerosols are problematic at low concentrations (high concentrations trigger the cloud mask). Gordon et al. (1997), Moulin et al. (2001), and Banzon et al. (2004) outline and apply a "spectral matching" approach to the problem. However, the methodology is computationally intensive and integration with the standard processing technique of Gordon and Wang is problematic. Rather than correct for aerosol absorption, simply detecting and excluding contaminated pixels would suffice. Nobileau & Antoine (2005) outlined an approach based on reflectance at 510 nm in Case 1 waters (reflectance dominated by pigment absorption), although extensive validation by the NASA Ocean Biology Processing Group, in collaboration with the authors, yielded unsatisfactory results. Recently, Ahmad et al. (2007) devised an NO_2 absorption correction scheme that improves water-leaving radiance retrievals at 412 and 443 nm in coastal regions affected by air pollution. Finally, Morel et al. (2002) summarized their modeling investigations of the ocean bidirectional reflectance and a procedure for normalizing satellite-derived water-leaving radiances from various solar and observation geometries to the nadir direction.

Empirical bio-optical algorithms based on water-leaving radiance ratio regressions against in situ water constituent concentrations or properties, e.g., chlorophyll *a* (O'Reilly et al. 1998) and diffuse attenuation coefficients [$K(\lambda)$], are markedly improved and several new products have been validated [calcite, particulate organic carbon, fluorescence line height (FLH)], although turbid coastal waters remain a challenge because of noncovariance of optical constituents (IOCCG, 2000). Semianalytical algorithms based on theoretical relationships between reflectance and inherent optical properties (IOPs; absorption and scattering coefficients) are now commonly used to invert the satellite reflectances to estimate the IOPs, e.g., by Garver & Siegel (1997), Carder et al. (1999), and Hoge et al. (1999). Because these models explicitly separate chlorophyll *a* and CDOM concentrations, semianalytical model chlorophyll *a* values can be significantly different from those derived using empirical algorithms (Siegel et al. 2005b, Hu et al. 2006)

and provide a means of estimating colored dissolved detrital and dissolved materials (CDM) (Siegel et al. 2002b) and particulate backscattering coefficients (Siegel et al. 2005a, Loisel et al. 2006). However, the inversions require accurate water-leaving radiances across the visible spectrum to perform adequately, and are generally tuned for open ocean applications or specific coastal regions, e.g., Magnuson et al. (2004). To avoid the decoupling of the aerosol and ocean reflectance calculations, methods for simultaneously deriving these have been developed. For example, Chomko et al. (2003) used a set of 72 aerosol models, including absorbing aerosols, with the Maritorena et al. (2002) ocean reflectance model (a revision of Garver & Siegel 1997) to formulate a "spectral optimization" technique and successfully tested it using SeaWiFS data off the U.S. east coast. This and similar methodologies are computationally intensive.

The satellite data product accuracy goals generally accepted by the international missions are $\pm 5\%$ for water-leaving radiances and $\pm 35\%$ for chlorophyll *a* in the open ocean. A number of evaluations have been published, including global analyses by Gregg & Casey (2004) (SeaWiFS chlorophyll *a*) and Bailey & Werdell (2006) [SeaWiFS water-leaving radiances, chlorophyll *a*, and K(490)]. Zibordi et al. (2006) compared SeaWiFS, MODIS, and MERIS water-leaving radiances to SeaPRISM observations from the *Acqua Alta* tower. Overall, these results indicate quite good performance. However, regional differences can be large. For instance, Mitchell & Holm-Hansen (1991) found the standard CZCS pigment algorithm underestimated concentrations near the Antarctic Peninsula by 50–70%, citing regional differences in pigment specific absorption and scattering as the cause. A number of recent investigations have provided new assessments (Moore et al. 1999, Arrigo & van Dijken 2004, Garcia et al. 2005) that are inconsistent. Marrari et al. (2006) suggest that the problem lies in the pigment measurement methodology, i.e., fluorometric versus high-pressure liquid chromatography (HPLC): HPLC-derived pigments agree with the standard satellite chlorophyll *a* product, but others point to regional differences in the dominant phytoplankton species (Garcia et al. 2005).

SCIENTIFIC APPLICATIONS: RECENT ACCOMPLISHMENTS

Many applications of ocean color data were exploited using the CZCS data sets, especially for certain coastal regions where time series over one or more annual cycles were collected. Since the launch of the OCTS, many publications have expanded and refined those analyses. However, because the more recent data sets have been used in new and different applications, I highlight these in the following sections. It is difficult to categorize uniquely the broad variety of ocean color research results, so I focus on a few topics where a number of papers clearly demonstrate a new emphasis.

Physical and Biological Interaction

Ocean biology is strongly influenced by physical properties (temperature, salinity, light) and dynamics (mixing, upwelling, advection). Unlike during the CZCS period, accurate global sea surface temperature, wind speed, sea level, and chlorophyll *a* time series are readily available for correlative analyses. Doney et al. (2003), Wilson & Adamec (2002), Yoder & Kennelly (2003), Uz & Yoder (2004) and Wilson & Coles (2005) provide detailed statistical analyses of the global biological variability in the context of physical dynamics.

Specific examples of large-scale interactions include observations by Goes et al. (2005), who investigated interannual changes in Arabian Sea summertime chlorophyll *a* concentrations and associated a 300% increase in offshore concentrations between 1997 and 2003 with changes in the monsoonal winds. This group related the wind field changes to Eurasian landmass warming and decreased snow cover. McClain et al. (2004b) and Gregg et al. (2005) showed that several

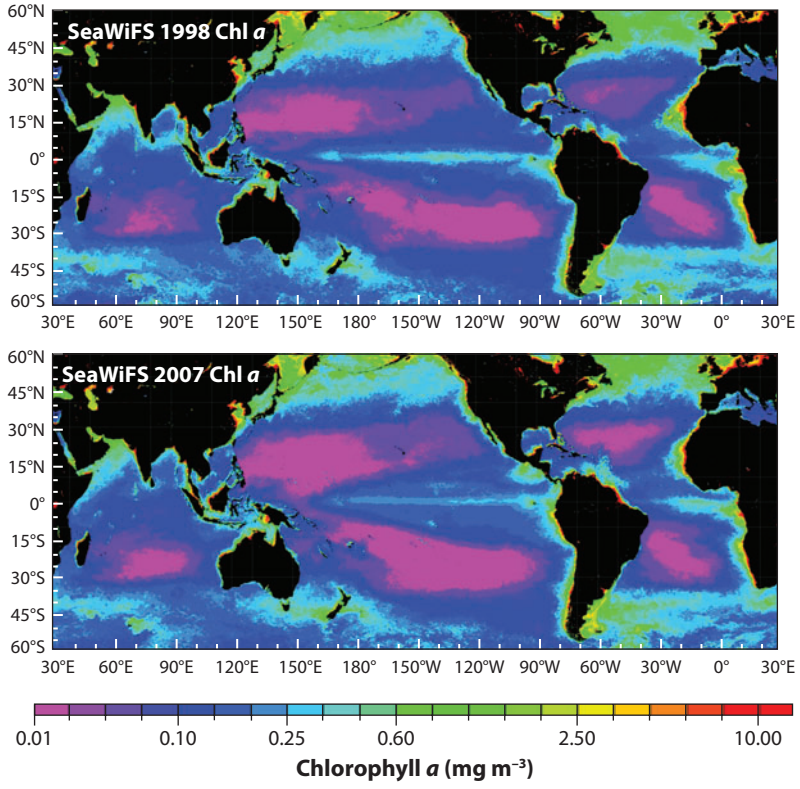

Figure 2

Sea-viewing Wide Field-of-view Sensor (SeaWiFS) global mean chlorophyll *a* concentrations for 1998 and 2007 showing the increased extent of the oligotrophic regions (*purple shades*) over a decade. Polovina et al. (2008) estimate the expansion to be approximately 15% between 1998 and 2006.

mid-ocean gyre systems have expanded during the early SeaWiFS record. These analyses have been extended by Polovina et al. (2008) using longer times series, which show that the expansions have continued and are more pronounced in the Southern Hemisphere than was initially reported (**Figure 2**). The expansion of oligotrophic waters was linked to higher sea surface temperatures (SSTs) in these studies.

Mesoscale open ocean processes.

Rossby waves. With routine high-resolution global coverage, some processes have been examined for the first time. For instance, several studies on Rossby wave signatures in the chlorophyll *a* global composites have been published (Cipollini et al. 2001, Uz et al. 2001, Charria et al. 2003, Dandonneau et al. 2003, Killworth 2004, Killworth et al. 2004). There has been some debate on the exact mechanism that produces the patterns (Dandonneau et al. 2004); proposals include biomass enhancements associated with wave-induced surface divergence (upwelling) and surface convergence (accumulation).

Mesoscale eddies. In the early 1980s, an intensive field study of Gulf Stream warm core rings was the first major program to be supported by satellite ocean color observations (Brown et al. 1985).

More recently, the influence of eddies in the Sargasso Sea has been the focus of modeling and observational studies in conjunction with the BATS program. McGillicuddy et al. (2001) showed the anticorrelation between satellite SST and chlorophyll images. In cyclonic eddies, isopycnals and the nutricline are uplifted, resulting in increased biomass and pigment concentrations that are detectable even at the surface. McGillicuddy et al. (2007) expand on this theme by including mode water eddies, which encompass a subsurface lens of water that hydrographically resemble a hybrid between cyclonic and anticyclonic eddies, i.e., upwelling isopycnals on the top of the lens and downwelling isopycnals below. These authors demonstrated that wind-eddy circulation interactions can enhance nutrient fluxes in anticyclonic and mode water eddies, but retard upwelling in cyclonic eddies. Siegel et al. (2008) provide additional observational evidence supporting this eddy-Ekman coupling.

New production: primary production supported by nitrate, usually mixed or upwelled from depth, or via the biological fixation of dinitrogen gas

Sverdrup critical depth and mixing. The classical model for events such as the North Atlantic spring bloom ties wintertime deep mixing to preconditioning the water column for blooms in spring when light and stratification levels become favorable for net growth of the phytoplankton community. Sverdrup (1953) synthesized this balance using the critical depth concept, i.e., the depth at which growth balances losses. Obata et al. (1996) used climatological mixed layer depths and CZCS pigment distributions to evaluate the Sverdrup criteria and seasonal pigment variability and found generally good agreement, with notable exceptions. Siegel et al. (2002a) focused on the North Atlantic spring bloom and the estimation of community compensation irradiance, one of the parameters in the Sverdrup formulation. This group estimated fairly uniform values across the basin above 40°N, but the magnitude was approximately twice that required by phytoplankton alone. Follows & Dutkiewicz (2002) examined three spring blooms (1998–2000) in the subtropical and subpolar North Atlantic to test the relationships between winter mixed layer depth (h_m), spring critical depth (h_c), heat fluxes, turbulent kinetic energy, the rate of wind work (friction velocity cubed) and chlorophyll. These authors found that the h_c:h_m ratio is a useful discriminator for determining whether mixing enhances (subtropics, high ratios) or retards (subpolar, low ratios) the bloom.

Storm-induced effects. Signatures of hurricane tracks on SST have been observed in satellite infrared imagery since the 1980s, but only recently have such signatures been identified in passive visible radiometry. Hoge & Lyon (2002) used their reflectance inversion methodology to identify CDOM absorption traces across the Sargasso Sea in the wake of Hurricane Gert in 1999. This signal persisted for up to 30 days. Babin et al. (2007) examined 13 hurricanes that traversed the Sargasso Sea from 1998–2001 using standard SeaWiFS chlorophyll *a* products: They found increases of chlorophyll *a* from 5% to 91%. In the majority of cases, they interpreted these increases as due to nutrient entrainment and phytoplankton growth, not just mixing of the deep chlorophyll *a* maximum, because of the 2–3 week persistence of these signatures. Siswanto et al. (2007) derived an algorithm to estimate the effect of typhoons on East China Sea outer shelf primary production. The algorithm parameters were maximum sustained wind speed, transit speed, and bottom depth. They correlated the typhoon-induced primary production enhancement to the Southern Oscillation Index (SOI) and found an inverse relationship, i.e., negative SOI corresponds with positive production enhancement. The connection to El Niño is due to the tendency of typhoons to be more frequent and intense during the tropical warm phase. These authors concluded that typhoon-induced new production accounted for up to 40% of the summer-fall new production (production supported by nitrate) and that decadal scale variations exist, i.e., typhoons had more impact during 1991–2004 than during 1980–1990.

1997–1998 El Niño–La Niña. The in situ and CZCS coverage of the 1982–1983 El Niño–La Niña was sparse, but some satellite ocean biology studies were published that highlighted biological responses, e.g., correlations between pigment concentration and sea level (Leonard & McClain 1996). The 1997–1998 El Niño–La Niña (**Figure 3**) was the most intense on record, surpassing even the 1982–1983 event. By this time, the TOGA (Tropical Ocean Global Atmosphere) Ocean-Atmosphere (TAO) array was in place along with ocean color and other satellite ocean sensors. The OCTS recorded the initial period of the warm phase (Murakami et al. 2000) in early 1997, and by the end of the OCTS record in June, chlorophyll *a* had decreased by 40% in the central equatorial Pacific. Chavez et al. (1999) provide the first overview of both the warm and cold phases, including estimates of iron fluxes, primary production, and CO_2 fluxes. They also provided one of the first SeaWiFS chlorophyll *a* validation data sets, indicating excellent agreement with field observations. The chlorophyll *a* concentrations in the central equatorial Pacific increased from

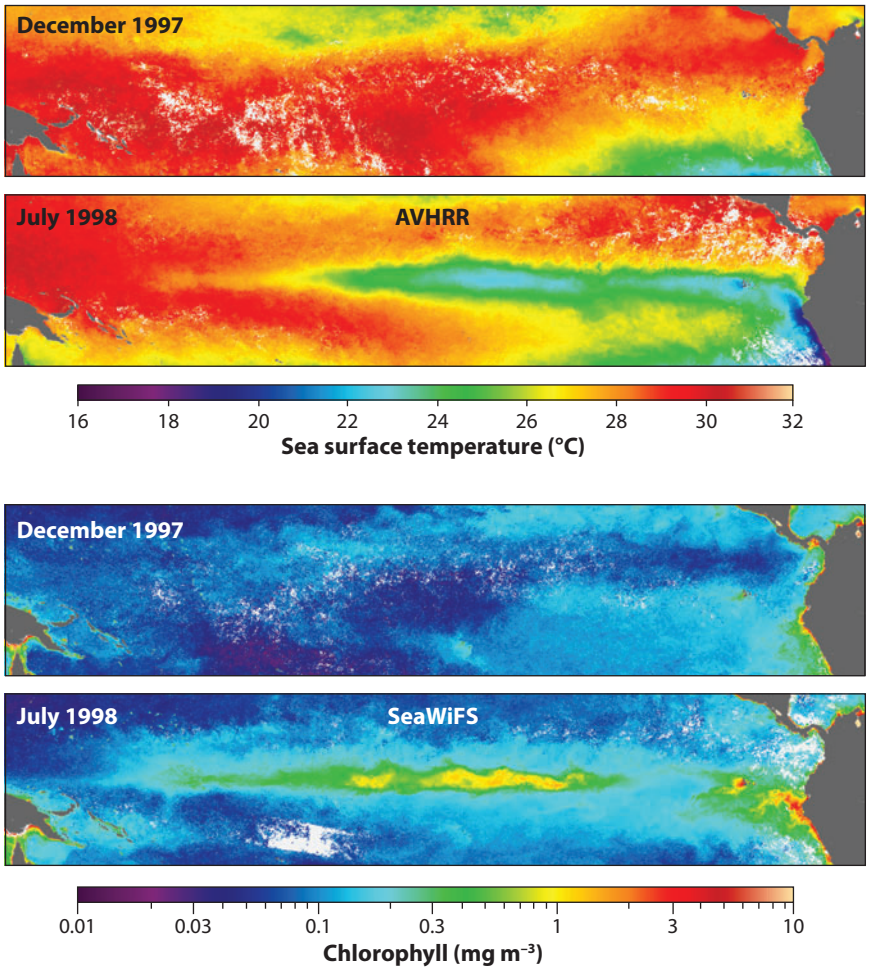

Figure 3

Monthly mean Advanced Very High Resolution Radiometer (AVHRR) sea surface temperatures (SST) and Sea-viewing Wide Field-of-view Sensor (SeaWiFS) chlorophyll *a* images during the warm (December 1997) and cold (July 1998) phases of the 1997–1998 El Niño–La Niña in the equatorial Pacific Ocean.

~0.2 mg/m^3 at the height of the warm phase in late 1997 to more than 1 mg/m^3 (the highest ever observed) during the cold phase in the summer of 1998. Murtugudde et al. (1999) considered not only the equatorial Pacific, but also the equatorial Indian Ocean response, incorporating satellite measurements of sea surface height and model simulations. These authors noted the elevated chlorophyll *a* values during the warm phase near 11°N and a 3° northward shift of the equatorial divergence zone by the end of the warm phase. They also pointed out the enhanced upwelling and chlorophyll *a* concentrations in the eastern tropical Indian Ocean and off Somalia during the warm phase. Wilson & Adamec (2001) compared the sea surface height and chlorophyll *a* fields and noted that the recommencement of the equatorial undercurrent (EU) occurred several months prior to the onset of La Niña. The inference is that the EU is the primary source of iron that eventually supported the La Niña bloom, as was suggested by Chavez et al (1999). This group also tied the elevated thermocline in the western equatorial Pacific to increased chlorophyll *a* during El Niño.

The La Niña onset was very sudden, e.g., SST dropped 6°C in the central equatorial Pacific in June 1998. This rapid transition resulted in an intense phytoplankton bloom that migrated from near 160°W to the South American coast between June and August (Strutton et al. 2001, McClain et al. 2002, Ryan et al. 2002). By its shape, the bloom clearly was associated with equatorial waves, e.g., tropical instability waves, and weekly chlorophyll *a* composites showed the eastward progression of the bloom.

Carr et al. (2002) provided a detailed description of the influence of the El Niño–La Niña on the South American coast using OCTS, SeaWiFS, sea level, coastal winds, and SST data. These authors found that the most pronounced decrease in chlorophyll *a* occurred off northern Chile. Kahru & Mitchell (2000) reported reduced coastal upwelling and chlorophyll *a* off southern California during the El Niño, similar to that observed using the CZCS data during the 1982–1983 El Niño, but increased chlorophyll *a* off Baja California. They suggest that the Baja bloom was caused by nitrogen-fixing cyanobacteria.

Net primary production (NPP): the net fixation of inorganic carbon by photosynthesis minus phytoplankton respiration

VGPM: vertically generalized production model

CbPM: carbon-based production model

Primary Production and Particulate Carbon

One of the principal applications of satellite ocean color data is to derive net primary production (NPP). Behrenfeld et al. (2002) provide a basic overview of photosynthesis and the basis for NPP algorithms such as the commonly used Behrenfeld & Falkowski (1997) formulation, the vertically generalized production model (VGPM). A wide variety of NPP algorithms exists and these have been assessed through a series of algorithm round-robins; Carr et al. (2006) is the most recent for global applications. These authors considered 24 different satellite algorithms whose mean annual production was 51 Gt C/yr. Because of the difficulties in specifying physiological variability in response to changing light, nutrient, and temperature conditions, usually parameterized as P_b^{opt} in these models, Behrenfeld et al. (2005) developed the carbon-based production model (CbPM), wherein determinations of particulate backscatter coefficients (b_{bp}) are used to estimate phytoplankton carbon (C) and growth rates (μ) are derived from chlorophyll:C ratios (**Figure 4**), thereby avoiding the need for an empirical physiological parameter (P_b^{opt}). A comparison of the VGPM and CbPM showed large zonal differences: The CbPM yielded a somewhat higher global average. Recently, Westberry et al. (2008) refined the model to include vertical variations in C and chlorophyll and estimated a global production at 52 Gt C/yr.

Satellite-based investigations for NPP range from regional to global assessments. Arrigo & van Dijken (2004) show that biological production in the Ross Sea is reduced by approximately 40% in years of heavy sea-ice cover such as 1997–1998 during the El Niño as compared with more normal years. In a previous study, Arrigo et al. (1998) used CZCS pigments to estimate annual production in the Southern Ocean (south of 50°S) at 4.4 Gt C/yr, which was four to five times higher than

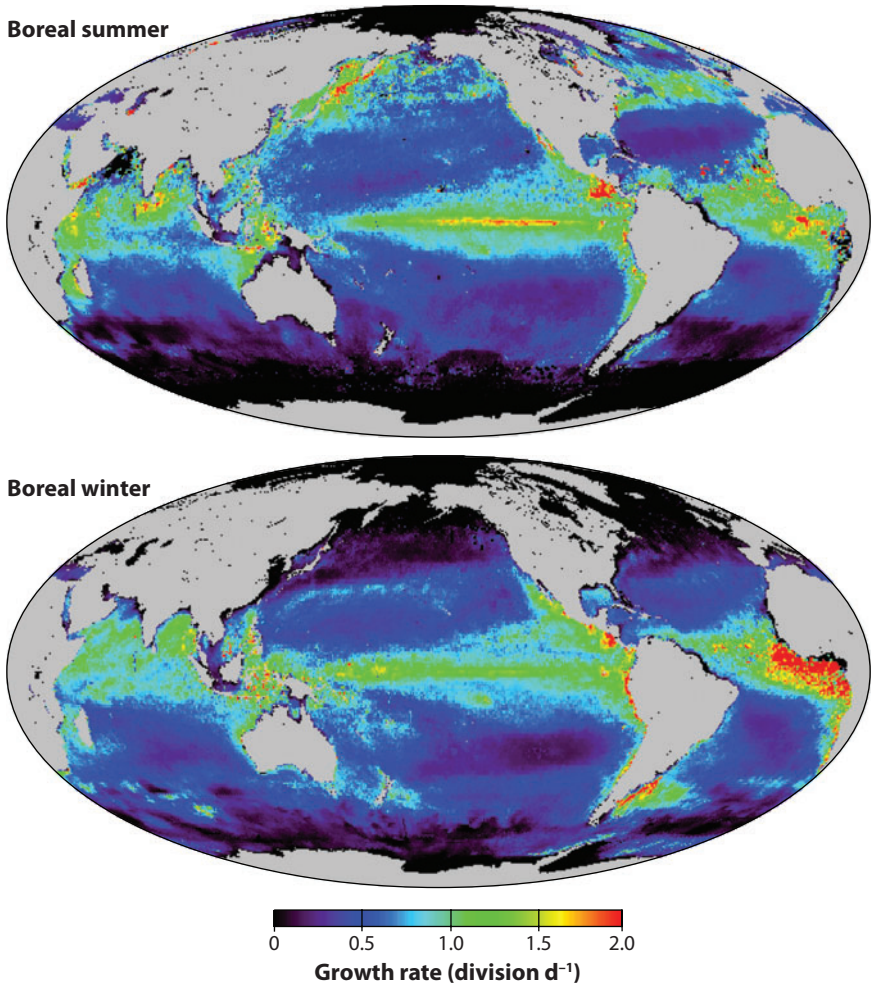

Figure 4

Global monthly mean phytoplankton growth rates (divisions per day) during the warm (*top*) and cold (*bottom*) phases of the 1997–1998 El Niño–La Niña derived from the carbon-based productivity model (CbBM). Figure provided by Mike Behrenfeld (Oregon State University).

previous estimates and consistent with the production required to support current inventories of upper trophic level biomass. Moore & Abbott (2000) used SeaWiFS data for the same domain and estimated production at 2.9 Gt C/yr. Some of the difference between their estimate and the higher Arrigo et al. (1998) value was attributed to the use of CZCS pigment rather than chlorophyll *a*.

Goes et al. (1999, 2000) outlined an approach for estimating surface nitrate and new production on the basis of in situ data in the North Pacific. These empirical relationships can then be applied to satellite SST and chlorophyll *a* data from that region for basin-scale assessments. Goes et al. (2004) applied this approach to five years of SeaWiFS and found that new production is higher in the northwestern portion of the basin and noticeable changes in annual new production correlate with winter wind speeds, e.g., 1998 (relatively high) versus 2001 (relatively low).

Behrenfeld et al. (2001) estimated the global primary productivity (ocean and terrestrial) for the period of September 1997–August 2000, the first three years of SeaWiFS coverage spanning

the El Niño–La Niña. This group concluded that overall annual oceanic productivity increased from approximately 54 to 59 PgrC/yr or roughly 10%, while terrestrial production varied little (~57.5 PgrC/yr), although large regional changes were observed.

A number of studies have evaluated decadal scale variations in primary production. Behrenfeld et al. (2006) showed that after the transition from low to high global production during the 1997–1998 El Niño–La Niña, production at low and mid-latitudes during 1999 through 2005 steadily declined as surface stratification increased. The mean chlorophyll *a* concentrations in this domain have rebounded somewhat from a low in late 2004 (Behrenfeld et al. 2008). Behrenfeld and coworkers also derived chlorophyll:C ratios from b_{bp} and separated its dependencies on photoclimation and nutrient-temperature stress. Their analysis shows that changes during the El Niño–La Niña of chlorophyll *a* in the permanently stratified oceans were due to changes in biomass, but subsequent changes are due to pigmentation. Furthermore, changes in the chlorophyll:C ratio were dominated by photoacclimation during 1997–2004, but nutrient-temperature stress was primary from 2005–2007.

Gregg & Conkright (2002) analyzed regional differences between the CZCS and SeaWiFS (1997–2000) global chlorophyll *a* distributions (satellite data with blended in situ data) and noted high latitude decreases and low latitude increases over time. Gregg et al. (2003a) compared global production differences between the early 1980s and the early years of the SeaWiFS mission (1997–2002) and estimated a 6% decrease, with most of the decline occurring at high latitudes. However, Antoine et al. (2005) suggest a 22% increase in chlorophyll *a* concentrations due mostly to changes at low latitudes. These two analyses were based on fundamentally different processing approaches that were applied to both sensors for consistency. These results underscore the importance of the international science community converging on processing algorithms and collaborating on product validation.

Calcite, a form of precipitated calcium carbonate, and particulate organic carbon have recently been established as standard archive products for NASA missions. Calcite, generally associated with coccolithophores, is a component of the particulate inorganic carbon (PIC) pool. Gordon et al. (2001) formulated an initial algorithm that accounted for the anomalously high surface reflectance effects on the aerosol correction, i.e., the calcite is derived using an alternative atmospheric correction and is processed separately from the other standard products. Balch et al. (2007) have refined the algorithm using a larger in situ data set collected during AMT cruises.

Particulate organic carbon (POC) is also a key component of the marine carbon cycle. Earlier work focused on regional analyses, but more recent global studies have become possible as POC databases have grown. Stramski et al. (1999) related the remote sensing reflectance at 555 nm, $R_{rs}(555)$, to POC via relationships to the particulate backscatter coefficient at 510 nm, $b_{bp}(510)$. Using SeaWiFS data, these authors estimated the POC south of 40°S at 0.8 Gt. Mishnov et al. (2003) used particulate beam-c (c_p) and POC data from the JGOFS North Atlantic Bloom Experiment and BATS and noncurrent SeaWiFS water-leaving radiance and POC data from the South Atlantic Ventilation Experiment (SAVE; 1987–1989) to derive an algorithm for POC in the South Atlantic. Loisel et al. (2002) used empirical relationships between total particulate backscatter (b_p) as a function of chlorophyll *a* and POC as a function of b_p to estimate the total surface POC at 19 Tg C/m (mean surface concentration times the total area) between 60°N–60°S. Using data from the polar North Atlantic, Stramska & Stramski (2005) evaluated five different algorithms and concluded that a normalized water-leaving radiance ratio, $L_{wn}(443)/L_{wn}(555)$, provided the best overall correlation with POC. These authors found that the seasonal range in POC for this region was <50 mg C/m^3 to approximately 400 mg C/m^3. Recently, Gardner et al. (2006) and Stramski et al. (2008) conducted global analyses. Basically, Gardner et al. extended the approach of Mishnov et al. using a larger data set, but estimated c_p from K(490). These researchers also derived

PIC: particulate inorganic carbon

POC: particulate organic carbon

chlorophyll:POC and c_p:chlorophyll fields. Chlorophyll:POC values ranged from approximately 0.1 in the mid-ocean gyres to >2 in coastal regions. Stramski et al. examined both empirical radiance ratio and two-step algorithms. The two-step algorithms used semianalytic inversions to derive particulate backscatter coefficients and then related these to POC. These authors found the empirical algorithms performed best overall.

Export production: the downward flux of biologically fixed carbon out of the ocean surface layer

Laws et al. (2000) developed an export production (the flux of organic carbon out of the surface layer) model dependent on net primary production and temperature. Using the advanced very high resolution radiometer (AVHRR) SST and SeaWiFS chlorophyll *a* products with the VGPM for production, these authors predicted a ~20% global average for export production with the highest values at high latitudes. Muller-Karger et al. (2005) modeled NPP and particle flux to estimate export production. According to their analyses, shelves account for 10–15% of global production and 40% of the global export flux reaching the bottom occurs on continental shelves. Lutz et al. (2007) looked at global seasonal cycles of NPP and POC fluxes using satellite and sediment trap data sets. This group found that the efficiency of the biological pump is reduced during bloom conditions, i.e., the flux is reduced relative to the primary production and that production variability versus latitude is greater than that of the particle fluxes.

Ecosystem Composition

Understanding ecosystem dynamics and biogeochemical cycles requires an understanding of the distribution and concentration of phytoplankton species or functional groups. Some species such as coccolithophores have very obvious signatures that are fairly easy to identify in the satellite imagery. When abundances are high, nitrogen-fixing *Trichodesmium* also has an optical signature that is anomalous from other phytoplankton. Also, as pigment databases are expanded to include phytoplankton chemotaxonomic pigment concentrations, the estimation of functional group abundance on the basis of pigment composition becomes possible. Given sufficient spectral information, estimates of pigment composition using reflectance inversion algorithms can be made, leading to estimation of functional groups. The existing sensors such as SeaWiFS provide a minimum number of bands in the visible for pigment separation, but some progress is being made.

Coccolithophores. Coccolithophores bloom in highly stratified waters, especially when nutrient concentrations and competition with other phytoplankton are low, e.g., the North Atlantic in summer (Raitsos et al. 2006). Coccolithophores shed calcium carbonate platelets that can turn the water an aquamarine color that is quite discernible in the unprocessed satellite imagery (Vance et al. 1998). Usually, this phenomenon allows the blooms to be flagged to avoid erroneous estimates of chlorophyll *a* concentrations and spatial and temporal distributions of flagged data have been used to study coccolithophore ecology (Brown & Yoder 1994). Calcite products are now available that are more quantitative for carbon cycle studies.

In 1997, a large persistent bloom of *Emiliania huxleyi* developed in the eastern Bering Sea (Vance et al. 1998, Iida et al. 2002). This was the first such bloom in the Bering Sea ever observed and it resulted in major die-offs of sea bird populations and a substantial reduction in the annual salmon run. Blooms during 1998–2001 were found to persist from approximately February into fall with peaks in April and September. Variability in the bloom extent from year to year seemed to be correlated with SSTs. Smyth et al. (2004) analyzed 20 years of data from the CZCS, the AVHRR, and SeaWiFS for coccolithophore blooms in the Barents Sea and suggested that bloom occurrence correlated with high temperature/low salinity anomalies that would become more frequent in a global warming scenario.

Using the calcite and chlorophyll *a* products from SeaWiFS, Signorini et al. (2006) showed the seasonal succession of phytoplankton species along the Patagonian shelf break in the vicinity of the northward flowing Malvinas Current. Early in the austral spring, a bloom develops along the shelf break. During this period, no coccolithophores are detected. By December, coccolithophores are clearly present and the shelf break chlorophyll *a* concentrations are much lower. This sequence suggests a succession of dominant phytoplankton groups beginning with spring blooms of primarily diatoms when nutrients and light are high and the water column is somewhat stratified. Later, after surface nutrients are reduced and stratification is much increased, coccolithophores replace the previous population. This pattern was consistently repeated over the eight-year study, but with considerable variability in the seasonal chlorophyll *a* and calcite peak concentrations.

***Trichodesmium*.** Nitrogen fixation by cyanobacteria is an important process in the marine nitrogen cycle, especially where nitrate is limited, although it has a high iron requirement that imposes limits. Subramaniam et al. (1999a, 1999b) provided much of the impetus for pursuing the identification of *Trichodesmium* blooms in satellite imagery based on observations of absorption spectra and marine reflectance modeling. This work was followed with case studies of field and satellite observations that confirmed the blooms could be uniquely detected (Dupouy et al. 2000, Subramaniam et al. 2002). The bloom detection algorithm was improved by Westberry et al. (2005), who determined a detection threshold of 3200 trichomes/liter. Westberry & Siegel (2006) subsequently applied the algorithm to weekly averaged SeaWiFS water-leaving radiances for 1998–2003 to estimate time series of global *Trichodesmium* bloom occurrences. These authors found that blooms occur most frequently, more than 35% of the time, in the equatorial Pacific and the western Arabian Sea. They also estimated global rates of nitrogen fixation by *Trichodesmium* under nonbloom and bloom conditions at 20 and 42 Tg N/year, respectively. Capone et al. (1997) estimated nonbloom fixation at 80 Tg N/year.

Red tides and harmful algal blooms. The terms red tide and harmful algal blooms (HABs) have many connotations that can confuse the discussion. Stumpf & Tomlinson (2005) provide a useful overview of the topic and a basis for remote sensing detection of these blooms. Because HABs are relatively infrequent and short lived, few studies using the CZCS data were published, e.g., Paláez (1987). However, with routine coverage, monitoring for HABs and red tides is possible. Kahru & Mitchell (1998) used spectral reflectance and absorption measurements from a red tide off southern California to show that bands between 340–400 nm are needed to accurately distinguish between these and more typical phytoplankton blooms. Only the GLI has such bands at 380 and 400 nm.

Much work on satellite detection of HABs has been focused on the west Florida shelf because *Karenia brevis* blooms are common. The Monitoring and Event Response for Harmful Algal Blooms (MERHAB), the Ecology and Oceanography of Harmful Algal Blooms (ECOHAB), and the Hyperspectral Coastal Ocean Dynamics Experiment (HyCODE) have provided in situ data for testing methodologies. One method designed for sensors such as SeaWiFS without the UV bands is based on chlorophyll *a* anomalies (Stumpf et al. 2003, Tomlinson et al. 2004) and has been used by the National Oceanic and Atmospheric Administration (NOAA) for HABs alerts. Problems in the chlorophyll *a* anomaly approach due to resuspension of benthic chlorophyll *a* are addressed in Wynne et al. (2005). On the basis of in situ data, Cannizzaro et al. (2008) found that *Karenia brevis* blooms have a significantly reduced backscatter to chlorophyll *a* ratio [$b_b(555)$/chl-a] compared with that of the background phytoplankton community, suggesting an alternative approach. However, because of errors associated with the atmospheric correction and CDOM absorption in coastal waters, the satellite spectral inversion techniques and empirical chlorophyll *a* retrievals are presently too inaccurate to reliably identify HABs using only this ratio (Hu et al.

2008). Cannizzaro et al. did examine MODIS FLH for discriminating between high CDOM and high chlorophyll *a* waters. This approach also minimizes atmospheric correction errors because the extrapolation of aerosol radiance from the NIR bands to the FLH bands is less extreme. However, Gilerson et al. (2008a, 2008b) show that the FLH signal is masked by particulate backscattering in turbid water.

Functional groups. The spatial variability and concentration of various functional groups is important to understanding ecosystem composition and dynamics, improving primary production estimates, and quantifying the effects of climate change. Perhaps the first attempt at separating phytoplankton groups using satellite data was described in a report by Alvain et al. (2005). This group matched an in situ data set of 22 pigments from more than 1100 stations with coincident satellite L_{wn}s, resulting in a final set of 176 stations after quality control. This data set was then used to define a procedure for assigning spectral shapes to four dominant phytoplankton groups: haptophytes, *Prochlorococcus*, *Synechococcus*-like cyanobacteria (SLC), and diatoms. The algorithm was then applied to global SeaWiFS monthly water-leaving radiance fields, showing that *Prochlorococcus* and SLC dominate oligotrophic tropical waters, and haptophytes (winter) and diatoms (summer) dominate high-latitude eutrophic waters. Uitz et al. (2006) used more than 2400 open ocean pigment profiles to relate surface chlorophyll *a* concentrations to the relative abundances of picoplankton, nanoplankton, and microplankton size classes. Loisel et al. (2006) examined the spectral slope of $b_{bp}(\lambda)$ as an indicator of the particle size distribution, i.e., greater slopes are associated with smaller particles. The mid-ocean gyres stand out as areas of high spectral slope.

Ecosystem Model Data Assimilation

Remote sensing data provide information only on property distributions in the first optical depth of the water column, although statistical relationships can be used to infer vertical distributions of chlorophyll *a* (Uitz et al. 2006) and depth-integrated properties such as the euphotic depth (Morel et al. 2007) on the basis of surface chlorophyll *a* concentration. Numerical ecosystem models coupled to physical circulation models provide a much more complete description of the biogeochemistry of the ocean, depending on the complexity of the model. The more complex the model, the more process parameterizations and free variables to specify. Data assimilation techniques can be used not only to constrain the model to track observational time series, but also to optimize certain variables.

In one of the earliest attempts, Ishizaka (1990) inserted CZCS pigment values from a short sequence of images of Gulf Stream frontal eddies off northeast Florida into a simple four-component ecosystem model with advection derived from an array of moored current meters. In this highly variable study domain, the simulation fidelity rapidly degenerated to the model result without assimilation. Armstong et al. (1995) used a 13-component ecosystem model of the North Atlantic forced by a general circulation model to test a model "nudging" technique using CZCS monthly pigment climatologies. Model estimates of chlorophyll *a* concentration were substantially improved and basin-scale estimates of primary production were reduced by a factor of two or more with data assimilation.

With the more frequent global coverage of SeaWiFS, data assimilation is much more feasible over a greater diversity of ecosystems. Friedrichs (2001) compared the performance of data insertion and a variational adjoint method in the equatorial Pacific using a one-dimensional five-component ecosystem model with field and satellite data and evaluated the effects of random noise and biases in the data. Friedrichs (2002) then evaluated parameter optimization using the adjoint method for the same study region and ecosystem model. Her studies emphasize the fact that the

model complexity must reflect that of the actual ecosystem. Garcia-Gorriz et al. (2003) also used the variational adjoint method to assimilate SeaWiFS chlorophyll *a* data into a three-dimensional coupled ecosystem-dynamical model of the Adriatic Sea for January and June, 1998. The resulting uncertainties differed for the two months and for the north and south basins and were attributed to SeaWiFS sampling. Natvik & Evensen (2003a, 2003b) used the ensemble Kalman filter with a basin-scale three-dimensional coupled ecosystem-dynamical model of the North Atlantic spring bloom (April and May, 1998). Without assimilation, the model predicted blooms where blooms were not observed, but performance greatly improved with assimilation.

In a series of papers (Gregg & Conkright 2002, Gregg et al. 2003b, Gregg & Casey 2007), the development of a global three-dimensional coupled biogeochemical-physical model is outlined with SeaWiFS chlorophyll *a* fields serving as validation data. Assimilation of SeaWiFS chlorophyll *a* data into this model using the singular evolutive interpolated Kalman filter over seven years is described in Nerger & Gregg (2007). These authors showed a substantial reduction in model log error of chlorophyll, i.e., 0.32 with assimilation versus 0.43 without assimilation, when compared with in situ data. SeaWiFS chlorophyll *a* log error was cited as 0.28 when compared with the in situ data. Gregg (2008) applied the conditional relaxation analysis method to the same global model using SeaWiFS chlorophyll *a* data for six years (1998–2003) to show that the free-run model bias could be reduced from an annual global mean of 21% to 5.5% with daily assimilations. He also compared VGPM and model global production and found that the model overestimation (~21%) with respect to the VGPM (~40 Pg C/yr) was reduced by nearly 50% with data assimilation to ~45 Pg C/yr. Finally, Tjiputra et al. (2007) apply an adjoint method to a three-dimensional global coupled ocean biogeochemical-physical model using SeaWiFS chlorophyll *a* seasonal climatologies to evaluate the regional model sensitivity to various processes such as exudation, grazing, and fecal pellet egestion. These authors found that the assimilation improved model performance at high latitudes. The best set of regional parameters yielded global net primary production of 36 Pg C/yr.

Climate data record (CDR): a geophysical time series of sufficient length, consistency, and continuity to determine climate variability and change

FUTURE RESEARCH DIRECTIONS AND CHALLENGES FOR SATELLITE OCEAN BIOGEOCHEMISTRY

With the general acceptance of anthropogenic impacts on climate and coastal water quality, maintenance and continuity of the existing satellite ocean biogeochemical climate data records (CDRs) is a very high priority. SeaWiFS, MODIS, and MERIS are either well beyond or nearing the end of their design lives, and it is unclear how continuity will be achieved. Sensors with ocean color capabilities are scheduled for launch within the next two years, e.g., the Ocean Color Monitor (OCM-2, India) and the Visible-Infrared Imaging Radiometer Suite (VIIRS, United States). However, sensor performance and on-orbit sensor calibration stability will remain issues until at least a couple of years after launch, pending postlaunch validation. Overlap with the existing missions is essential to guarantee seamless time series across missions. To develop CDRs from a combination of international missions requires open access to all data, including the prelaunch characterization and on-orbit calibration data, but this does not ensure continuity of data quality and coverage.

The trend in ocean bio-optical algorithms is toward semianalytical models with inversion schemes to extract IOPs, which can then be used to estimate a variety of key biogeochemical parameters such as POC, particle size distributions, functional groups, and habitat identification. Currently, sensors such as SeaWiFS offer a minimal set of spectral bands for these inversions. To separate pigments such as CDOM and chlorophyll *a*, spectral bands below 412 nm are required. To derive accurate reflectances in turbid water, additional high-SNR bands in the SWIR are

required for the aerosol corrections. FLH is a product that has not been utilized much to date, but recent innovative work on FLH as an indicator of phytoplankton physiology is promising and applications in turbid water should be explored more extensively.

Finally, as the diversity and accuracy of the satellite products improve, data assimilation into coupled physical-biogeochemical models will continue to evolve and lead to a more accurate and detailed description of the interactions and fluxes. Data assimilation on global scales is computationally intensive, but is essential to refine process parameterizations and forecast ecosystem responses to weather and climate scenarios. However, to be useful for forecasting, continuity of high-quality satellite data is required.

SUMMARY POINTS

1. Second generation sensors such as SeaWiFS, MODIS, OCTS, GLI, and MERIS have taken the state of the art far beyond what the proof-of-concept CZCS mission could deliver. Of these, only the SeaWiFS sensor was designed specifically for ocean color science and the data it generates are currently considered the highest-quality ocean color data, attaining the requirements necessary for ocean biogeochemistry and climate research.
2. Advances in pre- and postlaunch calibration methodologies, such as the lunar calibration and the in situ (e.g., MOBY-based) vicarious calibration, were essential for the development of ocean biogeochemistry climate data records (CDRs).
3. Recent improvements in field observation capabilities and bio-optical algorithms (empirical and semianalytical) have provided the means to derive a variety of geophysical products such as chlorophyll *a* concentration, colored dissolved organic matter (CDOM), pigment absorption coefficients, particulate organic carbon (POC), calcite, and phytoplankton carbon, growth rates, and primary production.
4. Ocean color data products are being used to address a very wide assortment of investigations that range from global decadal trends in primary production and the distributions of phytoplankton functional groups to water quality issues in coastal zones.
5. Now that global products are routinely available, data assimilation of biological and biogeochemical parameters into global climate and coupled physical-ecosystem models is leading to improved simulations and a clearer understanding of where further model improvements are needed.

FUTURE ISSUES

1. Performance uncertainties for currently approved future ocean color sensors threaten the continuation of existing ocean biology and biogeochemistry CDRs beyond the limited life expectancy of the current heritage sensors.
2. Current and approved sensors [e.g., the Visible and Infrared Imaging Radiometer Suite (VIIRS)] will not provide the spectral information required to exploit recent advances in marine optics and bio-optics that will allow greater insight into the marine carbon cycle, unambiguous identification of phytoplankton functional groups and harmful algal blooms (HABs), and accurate products in turbid (nearshore and estuarine) waters. The next-generation sensors must incorporate additional bands in the ultraviolet (UV), visible, near-infrared (NIR) and shortwave-infrared (SWIR).

3. The expanded suite of data products required by the science community necessitates a well-organized and adequately funded calibration and validation program with international participation. Such a program does not exist at this time.
4. All international organizations supporting missions with ocean color sensors must ensure unrestricted access to in situ and satellite ocean color data at all data levels, including satellite prelaunch characterization and on-orbit calibration data. Without this, a data consistency/quality gap, if not a mission coverage gap, will almost certainly occur, which will inhibit understanding of the impacts of climate variability and change on ocean biogeochemistry and the role of the oceans in the Earth system.

DISCLOSURE STATEMENT

The author is not aware of any biases that might be perceived as affecting the objectivity of this review.

ACKNOWLEDGMENTS

The author would like to thank the *Annual Review of Marine Science* for the opportunity to provide this review and acknowledges Jim Aiken, David Antoine, Kevin Arrigo, Ichio Asunuma, Barney Balch, Mike Behrenfeld, Stan Hooker, Greg Mitchell, Dave Siegel, and Jim Yoder, who provided recommendations on citations to be considered in the review.

LITERATURE CITED

Abbott MR, Chelton DB. 1991. Advances in passive remote sensing of the ocean. *U.S. National Report to International Union of Geodesy and Geophysics 1987–1990, Contributions in Oceanography*, pp. 571–89, Am. Geophys. U.

Ahmad Z, McClain CR, Herman JR, Franz BA, Kwaitkowska EJ, et al. 2007. Atmospheric correction of NO_2 in retrieving water-leaving reflectances from the SeaWiFS and MODIS measurements. *Appl. Opt.* 46(26):6504–12

Alvain S, Moulin C, Dandonneau Y, Bréon FM. 2005. Remote sensing of phytoplankton groups in case 1 waters from global SeaWiFS imagery. *Deep-Sea Res. I* 52:1989–2004

Antoine D, d'Ortenzio F, Hooker SB, Bècu G, Gentili B, et al. 2008. Assessment of uncertainty in the ocean reflectance determined by three satellite ocean color sensors (MERIS, SeaWiFS, and MODIS-A) at an offshore site in the Mediterranean Sea (BOUSSOLE project). *J. Geophys. Res.* 113:C07013

Antoine D, Morel A, Gordon HR, Banzon VF, Evans RH. 2005. Bridging ocean color observations of the 1980s and 2000s in search of long-term trends. *J. Geophys. Res.* 110:C06009

Armstrong RA, Sarmiento JL, Slater RD. 1995. Monitoring ocean productivity by assimilating satellite chlorophyll into ecosystem models. In: *Ecological Time Series*, ed. TM Powell, JH Steele, pp. 371–90. London: Chapman & Hall. 514 pp.

Arrigo KR, van Dijken GL. 2004. Annual changes in sea-ice, chlorophyll *a*, and primary production in the Ross Sea, Antarctica. *Deep-Sea Res. II* 51:117–38

Arrigo KR, Worthen D, Schnell A, Lizotte MP. 1998. Primary production in Southern Ocean waters. *J. Geophys. Res.* 103(C8):15587–600

Babin SM, Carton JA, Dickey TD, Wiggert JD. 2007. Satellite evidence of hurricane-induced phytoplankton blooms in an oceanic desert. *J. Geophys. Res.* 109:C03043

Bailey SW, Werdell PJ. 2006. A multi-sensor approach for the on-orbit validation of ocean color satellite data products. *Remote Sens. Environ.* 102:12–23

Balch W, Drapeau D, Bowler B, Booth E. 2007. Prediction of pelagic calcification rates using satellite measurements. *Deep-Sea Res. II* 54:478–95

Banzon VF, Evans RE, Gordon HR, Chomko RM. 2004. SeaWiFS observations of the Arabian Sea southwest monsoon bloom for the year 2000. *Deep-Sea Res. II* 51:189–208

Barale V, Schlittenhardt PM. 1993. *Ocean Colour: Theory and Applications in a Decade of CZCS Experience*. Dordrecht/Boston/London: Kluwer. 347 pp.

Barnes RA, Eplee RE Jr, Patt FS, Kieffer HH, Stone TC, et al. 2004. Comparison of the on-orbit response history of SeaWiFS with the U.S. Geological Survey lunar model. *Appl. Opt.* 43(31):5838–54

Behrenfeld MJ, Boss E, Siegel DA, Shea DM. 2005. Carbon-based ocean productivity and phytoplankton physiology from space. *Global Biogeochem. Cycles* 19:GB1006

Behrenfeld MJ, Esaias WE, Turpie KR. 2002. Assessment of primary production at global scale. In *Phytoplankton Productivity: Carbon Assimilation in Marine and Freshwater Ecosystems*, ed. PJ le B. Williams, DN Thomas, CS Reynolds, pp. 156–86. Wiley-Blackwell. 400 pp.

Behrenfeld MJ, Falkowski PG. 1997. Photosynthetic rates derived from satellite-based chlorophyll concentration. *Limnol. Oceanogr.* 42(1):1–20

Behrenfeld MJ, Halsey KH, Milligan AJ. 2008. Evolved physiological responses of phytoplankton to their integrated growth environment. *Phil. Trans. Royal Soc. B* 363:2687–703

Behrenfeld MJ, O'Malley RT, Siegel DA, McClain CR, Sarmiento JL, et al. 2006. Climate-driven trends in contemporary ocean productivity. *Nature* 444(7):752–55

Behrenfeld MJ, Randerson JT, McClain CR, Feldman GC, Los SO, et al. 2001. Biospheric primary production during the ENSO transition. *Science* 291:2594–97

Brown CW, Yoder JA. 1994. Coccolithophorid blooms in the global ocean. *J. Geophys. Res.* 99(C4):7467–82

Brown O, Evans RH, Brown JW, Gordon HR, Smith RC, et al. 1985. Phytoplankton blooming of the U.S. east coast: a satellite description. *Science* 229:163–67

Cannizzaro JP, Carder KL, Chen FR, Heil CA, Vargo GA. 2008. A novel technique for detection of the toxic dinoflagellate, *Karenia brevis*, in the Gulf of Mexico from remotely sensed ocean color data. *Cont. Shelf Res.* 28:137–58

Capone DG, Zehr JP, Paerl HW, Bergman B, Carpenter EJ. 1997. *Trichodesmium*, a globally significant marine cyanobacterium. *Science* 276:1221–29

Carder KL, Chen FR, Lee ZP, Hawes SK, Kamykowski D. 1999. Semianalytic moderate-resolution imaging spectrometer algorithms for chlorophyll *a* and absorption with bio-optical domains based on nitrate-depletion temperatures. *J. Geophys. Res.* 104(C3):5403–21

Carr M-E, Friedrichs MAM, Schmeltz M, Aita MN, Antoine D, et al. 2006. A comparison of global estimates of marine primary production from ocean color. *Deep-Sea Res. II* 53(5–7):741–70

Carr M-E, Strub PT, Thomas AC, Blanco JL. 2002. Evolution of 1996–1997 La Niña and El Niño conditions off the western coast of South America: a remote sensing perspective. *J. Geophys. Res.* 107(C12):3236

Charria G, Mélin F, Dadou I, Radenac M-H, Garçon V. 2003. Rossby wave and ocean color: The cells uplifting hypothesis in the South Atlantic subtropical convergence zone. *Geophys. Res. Lett.* 30(3):1125

Chavez FP, Strutton PG, Friederich GE, Feely RA, Feldman GC, et al. 1999. Biological and chemical response of the equatorial Pacific Ocean to the 1997–98 El Niño. *Science* 286:2126–31

Chomko RM, Gordon GR, Maritorena S, Siegel DA. 2003. Simultaneous retrieval of oceanic and atmospheric parameters for ocean color imagery by spectral optimization: a validation. *Remote Sens. Environ.* 84:208–20

Cipollini P, Cromwell D, Challenor PG, Raffaglio S. 2001. Rossby waves detected in global ocean colour data. *Geophys. Res. Lett.* 28(2):323–26

Clark DK, Gordon HR, Voss KJ, Ge Y, Broenkow W, et al. 1997. Validation of atmospheric correction over the ocean. *J. Geophys. Res.* 102(D14):17209–17

Clarke GL, Ewing GC, Lorenzen CJ. 1970. Spectra of backscattered light from sea obtained from aircraft as a measure of chlorophyll concentration. *Science* 16:1119–21

Claustre H, Hooker SB, Van Heukelem L, Berthon J-F, Barlow R, et al. 2004. An intercomparison of HPLC phytoplankton pigment methods using in situ samples: application to remote sensing and database activities. *Mar. Chem.* 85:41–61

Dandonneau Y, Menkes C, Gorgues T, Madec G. 2004. Reponse to comment on "Oceanic Rossby waves acting as a 'hay rake' for ecosystem floating by-products." *Science* 304:390c

Dandonneau Y, Vega A, Loisel H, du Penhoat Y, Menkes C. 2003. Oceanic Rossby waves acting as a "hay rake" for ecosystem floating by-products. *Science* 302:1548–51
Doney SC, Glover DM, McCue SJ, Fuentes M. 2003. Mesoscale variability of sea-viewing wide field-of-view sensor (SeaWiFS) satellite ocean color: Global patterns and spatial scales. *J. Geophys. Res.* 108(C2):3024
Dupouy C, Neveux J, Subramaniam A, Mulholland MR, Montoya J, et al. 2000. Satellite captures Trichodesmium blooms in the southwestern tropical Pacific. *Eos, Trans. Am. Geophys. U.* 18(2):13
Follows M, Dutkiewicz S. 2002. Meteorological modulation of the North Atlantic spring bloom. *Deep-Sea Res. II* 49:321–44
Franz BA, Bailey SW, Werdell PJ, McClain CR. 2007. Sensor-independent approach to the vicarious calibration of satellite ocean color radiometry. *Appl. Opt.* 46(22):5068–82
Friedrichs MAM. 2001. A data assimilative marine ecosystem model of the central equatorial Pacific: Numerical twin experiments. *J. Mar. Res.* 59:859–94
Friedrichs MAM. 2002. Assimilation of JGOFS EqPac and SeaWiFS data into a marine ecosystem model of the central equatorial Pacific Ocean. *Deep-Sea Res. II* 49:289–319
Garcia CAE, Garcia VMT, McClain CR. 2005. Evaluation of SeaWiFS chlorophyll algorithms in the southwestern Atlantic and Southern Oceans. *Remote Sens. Environ.* 95:125–137
Garcia-Gorriz E, Hoepffner N, Ouberdous M. 2003. Assimilation of SeaWiFS data in a coupled physical-biological model of the Adriatic Sea. *J. Mar. Sys.* 40–41:233–252
Gardner WD, Mishonov AV, Richardson MJ. 2006. Global POC concentrations from in-situ and satellite data. *Deep-Sea Res. II* 53:718–740
Garver SA, Siegel DA. 1997. Inherent optical property inversion of ocean color spectra and its biogeochemical interpretation I. Times series from the Sargasso Sea. *J. Geophys. Res.* 102(C8):18607–25
Gilerson A, Zhou J, Hlaing S, Ioannou I, Schalles J, et al. 2008a. Fluorescence component in the reflectance spectra from coastal waters. Dependence on water composition. *Opt. Express* 15(24):15702–22
Gilerson A, Zhou J, Hlaing S, Ioannou I, Schalles J, et al. 2008b. Fluorescence component in the reflectance spectra from coastal waters. II. Performance of retrieval algorithms. *Opt. Express* 16(4):2446–60
Goes JI, Gomes HDR, Limsakul A, Saino T. 2004. The influence of large-scale environmental changes on carbon export in the North Pacific Ocean using satellite and shipboard data. *Deep-Sea Res. II* 51(1–3):247–79
Goes JI, Saino T, Oaku H, Ishizaka J, Wong CS, et al. 2000. Basin scale estimates of sea surface nitrate and new production from remotely sensed sea surface temperature and chlorophyll. *Geophys. Res. Lett.* 27(9):1263–66
Goes JI, Saino T, Oaku H, Jiang DL. 1999. A method for estimating sea surface nitrate concentrations from remotely sensed SST and chlorophyll *a*—A case study for the North Pacific Ocean using OCTS/ADEOS data. *IEEE Trans. Geosci. Remote Sens.* 37:1633–44
Goes JI, Thoppil PG, do R Gomes H, Fasullo JT. 2005. Warming of the Eurasian landmass is making the Arabian Sea more productive. *Science* 308:545–47
Gordon HR, Boyton GC, Balch WM, Groom SB, Harbour DS, et al. 2001. Retrieval of coccolithophore calcite concentration from SeaWiFS imagery. *Geophys. Res. Lett.* 28(8):1587–90
Gordon HR, Clark DK, Brown JW, Brown OB, Evans RH, et al. 1983. Phytoplankton pigment concentrations in the Middle Atlantic Bight: comparison of ship determinations and CZCS estimates. *Appl. Opt.* 22:20–36
Gordon HR, Du T, Zhang T. 1997. Remote sensing of ocean color and aerosol properties: resolving the issue of aerosol absorption. *Appl. Opt.* 36:8670–84
Gordon HR, Wang W. 1994. Retrieval of water-leaving radiance and aerosol optical thickness over the oceans with SeaWiFS: a preliminary algorithm. *Appl. Opt.* 33(3):443–52
Gregg WW, Casey NW, McClain CR. 2005. Recent trends in global ocean chlorophyll. *Geophys. Res. Lett.* 32:L03606
Gregg WW, Casey NW. 2004. Global and regional evaluation of the SeaWiFS chlorophyll data set. *Remote Sens. Environ.* 93:463–79
Gregg WW, Casey NW. 2007. Modeling coccolithophores in the global oceans. *Deep-Sea Res. II* 54:447–77
Gregg WW, Conkright ME, Ginoux P, O'Reilly JE, Casey NW. 2003a. Ocean primary production and climate: global decadal changes. *Geophys. Res. Lett.* 30(15):1809

Gregg WW, Conkright ME. 2002. Decadal changes in global ocean chlorophyll. *Geophys. Res. Lett.* 29(15):1730
Gregg WW, Ginoux P, Schopf PS, Casey NW. 2003b. Phytoplankton and iron: validation of a global three-dimensional ocean biogeochemical model. *Deep-Sea Res. II* 50:3143–69
Gregg WW. 2008. Assimilation of SeaWiFS ocean chlorophyll data into a three-dimensional global ocean model. *J. Mar. Sys.* 69:205–25
Hoge FE, Lyon PE. 2002. Satellite observation of chromophoric dissolved organic matter (CDOM) variability in the wake of hurricanes and typhoons. *Geophys. Res. Lett.* 29(19):1908
Hoge FE, Wright W, Lyon PE, Swift RN, Yungel JK. 1999. Satellite retrieval of inherent optical properties by inversion of an oceanic radiance model: a preliminary algorithm. *Appl. Opt.* 38(3):495–504
Hooker S, Zibordi G. 2005. Platform perturbations in above-water radiometry. *Appl. Opt.* 44(4):553–67
Hooker SB, Lazin G, Zibordi G, McLean S. 2002. An evaluation of above- and in-water methods for determining water-leaving radiances. *J. Atmos Oceanic Tech.* 19:486–515
Hooker SB, Maritorena S. 2000. An evaluation of oceanographic radiometers and deployment methodologies. *J. Atmos. Oceanic Tech.* 17:811–30
Hooker SB, McClain CR. 2000. The calibration and validation of SeaWiFS data. *Prog. Oceanogr.* 45:427–65
Hooker SB, Morel A. 2003. Platform and environmental effects on above-water determination of water-leaving radiances. *J. Atmos Oceanic Tech.* 20:187–205
Hu C, Lee Z, Muller-Karger FE, Carder KL, Walsh JJ. 2006. Ocean color reveals phase shift between marine plants and yellow substance. *IEEE Geosci. Remote Sens. Lett.* 3(2):262–66.
Hu C, Luerssen R, Muller-Karger FE, Carder KL, Heil CA. 2008. On the remote monitoring of *Karenia brevis* blooms of the west Florida shelf. *Cont. Shelf Res.* 28:159–176
Iida T, Saitoh SI, Miyamura T, Toratani M, Fukashima H, et al. 2002. Temporal and spatial variability of coccolithophore blooms in the eastern Bering Sea, 1998–2001. *Prog. Oceanogr.* 55:165–75
IOCCG. 2000. Remote Sensing of Ocean Colour in Coastal, and Other Optically-Complex, Waters. Rep. No. 3, ed. S Sathyendranath. Dartmouth, Can.
Ishizaka J. 1990. Coupling of coastal zone color scanner data to a physical-biological model of the southeastern U.S. continental shelf ecosystem. 3. Nutrient and phytoplankton fluxes and CZCS data assimilation. *J. Geophys. Res.* 95(C11):20201-12
Kahru M, Mitchell BG. 1998. Spectral reflectance and absorption of a massive red tide off southern California. *J. Geophys. Res.* 103(C10):21601–09
Kahru M, Mitchell BG. 2000. Influence of the 1997–98 El Niño on the surface chlorophyll in the California current. *Geophys. Res. Lett.* 27(18):2837–940
Killworth PD. 2004. Comment on "Oceanic Rossby waves acting as a 'Hay Rake' for ecosystem floating by-products." *Science* 304:390b
Killworth PD, Cipollini P, Uz BM, Blundell JR. 2004. Physical and biological mechanisms for planetary waves observed in satellite-derived chlorophyll. *J. Geophys. Res.* 109:C07002
Lavender SJ, Pinkerton MH, Moore GF, Aiken J, Blondeau-Patissier D. 2005. Modification to the atmospheric correction of SeaWiFS ocean colour images over turbid waters. *Cont. Shelf Res.* 25:539–55
Laws EA, Falkowski FP, Smith WO Jr, Ducklow H, McCarthy JJ. 2000. Temperature effects on export production in the open ocean. *Global Biogeochem. Cycles* 14(4):1231–46
Leonard CL, McClain CR. 1996. Assessment of interannual variation (1979–1986) in pigment concentrations in the tropical Pacific using the CZCS. *Int. J. Remote Sens.* 17(4):721–32
Loisel H, Nicolas J-M, Deschamps P-Y, Froun R. 2002. Seasonal and interannual variability of particulate organic matter in the global ocean. *Geophys. Res. Lett.* 29(24):2196
Loisel H, Nicolas J-M, Sciandra A, Stramski D, Poteau A. 2006. Spectral dependency of optical backscattering by marine particles from satellite remote sensing of the global ocean. *J. Geophys Res.* 111:C09024
Lutz MJ, Caldeira K, Dunbar RB, Behrenfeld MJ. 2007. Seasonal rhythms of net primary production and particulate organic carbon flux to depth describe the efficiency of biological pump in global ocean. *J. Geophys. Res.* 112:C10011
Magnuson A, Harding LW Jr, Mallonee ME, Adolf JE. 2004. Bio-optical model for Chesapeake Bay and the Middle Atlantic Bight. *Estuarine, Coastal Shelf Sci.* 61:403–24
Maritorena S, Siegel DA, Peterson AR. 2002. Optimization of a semianalytical ocean color model for global-scale applications. *Appl. Opt.* 41:2705–14

Marrari M, Hu C, Daly K. 2006. Validation of SeaWiFS chlorophyll a concentrations in the Southern Ocean: a revisit. *Remote Sens. Environ.* 105:367–75

McClain C, Hooker S, Feldman G, Bontempi P. 2006. Satellite data for ocean biology, biogeochemistry and climate research. *Eos, Trans. Am. Geophys. U.* 87(34):337

McClain CR, Christian JR, Signorini SR, Lewis MR, Asanuma I, et al. 2002. Satellite ocean-color observations of the tropical Pacific Ocean. *Deep-Sea Res. II* 49:2522–60

McClain CR, Feldman GC, Hooker SB. 2004a. An overview of the SeaWiFS Project and strategies for producing a climate research quality global ocean bio-optical time series. *Deep-Sea Res. II* 51(1–3):5–42

McClain CR, Signorini SR, Christian JR. 2004b. Subtropical gyre variability observed by ocean color. *Deep-Sea Res. II* 51(1–3):281–301

McGillicuddy DJ Jr, Anderson LA, Bates NR, Biddy T, Buesseler KO, et al. 2007. Eddy/wind interactions stimulate extraordinary mid-ocean plankton blooms. *Science* 316:1021–26

McGillicuddy DJ Jr, Kosnyrev VK, Ryan JP, Yoder JA. 2001. Covariation of mesoscale ocean color and sea-surface temperature patterns in the Sargasso Sea. *Deep-Sea Res II* 48:1823–36

Meister G, Abel P, Barnes R, Cooper J, Davis C, et al. 2003. Comparison of spectral radiance calibrations at oceanographic and atmospheric research laboratories. *Meterologia* 40:S93-96

Mishnov AV, Gardner WD, Richardson MJ. 2003. Remote sensing and surface POC concentration in the South Atlantic. *Deep-Sea Res. II* 50:2997–3015

Mitchell BG. 1994. Coastal zone color scanner retrospective. *J. Geophys. Res.* 99:7291–92

Mitchell BG, Holm-Hansen O. 1991. Bio-optical properties of Antarctic Peninsula waters: differentiation from temperate ocean models. *Deep-Sea Res.* 38:1009–28

Moore JK, Abbott MR. 2000. Phytoplankton chlorophyll distributions and primary production in the Southern Ocean. *J. Geophys. Res.* 105(C12):28709–22

Moore JK, Abbott MR, Richman JG, Smith WO, Cowles TJ, et al. 1999. SeaWiFS satellite ocean color data from the Southern Ocean. *Geophys. Res. Lett.* 26(10):1465–68

Morel A, Antoine D, Gentilli B. 2002. Bidirectional reflectance of oceanic waters: accounting for Raman emission and varying particle scattering phase function. *Appl. Opt.* 41(30):6289–306

Morel A, Huot Y, Gentili B, Werdell PJ, Hooker SB, et al. 2007. Examining the consistency of products derived from various ocean sensors in open ocean (Case 1) waters in the perspective of a multi-sensor approach. *Remote Sens. Environ.* 111:69–88

Moulin C, Gordon HR, Chomko RM, Banzon VF, Evans RH. 2001. Atmospheric correction of ocean color imagery through thick layers of Saharan dust. *Geophys. Res. Lett.* 28(1):5–8

Muller-Karger FE, Varela R, Thunell R, Luerssen R, Hu C, et al. 2005. The importance of continental margins in the global carbon cycle. *Geophys. Res. Lett.* 32:L01602

Murakami H, Ishizaka J, Kawamura H. 2000. ADEOS observations of chlorophyll *a* concentration, sea surface temperature, and wind stress change in the equatorial Pacific during the 1997 El Niño. *J. Geophys. Res.* 105(C8):19551–59

Murtugudde RG, Signorini SR, Christian JR, Busalacchi AJ, McClain CR, et al. 1999. Ocean color variability of the tropical Indo-Pacific basin observed by SeaWiFS during 1997–1998. *J. Geophys. Res.* 104(C8):18351–66

Natvik L-J, Evensen G. 2003a. Assimilation of ocean colour data into a biochemical model of the North Atlantic Part 1. Data assimilation experiments. *J. Mar. Sys.* 40–41:127–53

Natvik L-J, Evensen G. 2003b. Assimilation of ocean colour data into a biochemical model of the North Atlantic Part 2. Statistical analysis. *J. Mar. Sys.* 40–41:155–69

Nerger L, Gregg WW. 2007. Assimilation of SeaWiFS data into a global ocean-biogeochemical model using a local SEIK filter. *J. Mar. Sys.* 68:237–54

Nobileau D, Antoine D. 2005. Detection of blue-absorbing aerosols using near infrared and visible (ocean color) remote sensing observations. *Remote Sens. Environ.* 95:368–87

Obata A, Ishizaka J, Endoh M. 1996. Global verification of critical depth theory for phytoplankton bloom with climatological in situ temperature and satellite ocean color data. *J. Geophys. Res.* 101(C9):20657–67

O'Reilly, JE, Maritorena S, Mitchell BG, Siegel DA, Carder KL, et al. 1998. Ocean color chlorophyll algorithms for SeaWiFS. *J. Geophys. Res.* 103(C11):24937–53

Paláez J. 1987. Satellite images of a "red tide" episode off Southern California. *Oceanologica Acta* 10(4):403–10

Polovina JJ, Howell EA, Abecassis M. 2008. Ocean's least productive waters are expanding. *Geophys. Res. Lett.* 35:L03618

Raitsos DE, Lavender SJ, Pradhan Y, Tyrrell T, Reid PC, et al. 2006. Coccolithophore bloom size variation in response to regional environment of subarctic North Atlantic. *Limnol. Oceanogr.* 51(5):2122–30

Ryan JP, Polito PS, Strutton PG, Chavez FP. 2002. Unusual large-scale phytoplankton blooms in the equatorial Pacific. *Prog. Oceanogr.* 55:263–85

Siegel DA, Court DB, Menzies DW, Peterson P, Maritorena S, et al. 2008. Satellite and in situ observations of the bio-optical signatures of two mesoscale eddies in the Sargasso Sea. *Deep-Sea Res II* 55:1218–30

Siegel DA, Doney SC, Yoder JA. 2002a. The North Atlantic spring phytoplankton bloom and Sverdrup's critical depth hypothesis. *Science* 296:730–33

Siegel DA, Maritorena SA, Nelson NB, Behrenfeld MJ. 2005a. Independence and interdependencies of global ocean color properties: reassessing the bio-optical assumption. *J. Geophys. Res.* 110:C07011

Siegel DA, Maritorena S, Nelson NB, Behrenfeld MJ, McClain CR. 2005b. Colored dissolved organic matter and its influence on the satellite-based characterization of the ocean biosphere. *Geophys. Res. Lett.* 32:L20605

Siegel DA, Maritorena S, Nelson NB, Hansell DA, Lorenzi-Kayser M. 2002b. Global distribution and dynamics of color dissolved and detrital organic materials. *J. Geophys. Res.* 107(C12):3228

Siegel DA, Wang W, Maritorena S, Robinson R. 2000. Atmospheric correction of satellite ocean color imagery: the black pixel assumption. *Appl. Opt.* 39:3582–91

Signorini SR, Garcia VT, Piola AR, Garcia CAE, Mata MM, et al. 2006. Seasonal and interannual variability of calcite in the vicinity of the Patagonian shelf break (38°S–52°S). *Geophys. Res. Lett.* 33:L16610

Siswanto E, Ishizaka J, Yokouchi K, Tanabe K, Tan CK. 2007. Estimation of interannual and interdecadal variations of typhoon-induced primary production: A case study for the outer shelf of the East China Sea. *Geophys. Res. Lett.* 34:L03604

Smyth TJ, Tyrrell T, Tarrant B. 2004. Time series of coccolithophore activity in the Barents Sea, from twenty years of satellite imagery. *Geophys. Res. Lett.* 31:L11302

Stramska M, Stramski D. 2005. Variability of particulate organic carbon concentration in the north polar Atlantic based on ocean color observations with sea-viewing wide field-of-view sensor (SeaWiFS). *J. Geophys. Res.* 110:C10018

Stramski D, Reynolds RA, Babin M, Kaczmarek S, Lewis MR, et al. 2008. Relationships between the surface concentration of particulate organic carbon and optical properties in the eastern South Pacific and eastern Atlantic Oceans. *Biogeosciences* 5:171–201

Stramski D, Reynolds RA, Kahru M, Mitchell BG. 1999. Estimation of particulate organic carbon in the ocean from satellite remote sensing. *Science* 285:239–42

Strutton PG, Ryan JP, Chavez FP. 2001. Enhanced chlorophyll associated with tropical instability waves in the equatorial Pacific. *Geophys. Res. Lett.* 28(10):2005–8

Stumpf RP, Culver ME, Tester PA, Tomlinson M, Kirkpatrick GJ, et al. 2003. Monitoring *Karenia brevis* blooms in the Gulf of Mexico using satellite ocean color imagery and other data. *Harmful Algae* 2:147–60

Stumpf RP, Tomlinson MC. 2005. Remote sensing of harmful algal blooms. In *Remote Sensing of Coastal Aquatic Environments*, ed. RL Miller, CE Del Castillo, BA McKee, pp. 277–96. AH Dordrecht, The Netherlands: Springer. 347 pp.

Subramaniam A, Brown CW, Hood RR, Carpenter EJ, Capone DG. 2002. Detecting *Trichodesmium* blooms in SeaWiFS imagery. *Deep-Sea Res. II* 49:107–21

Subramaniam A, Carpenter EJ, Falkowski PG. 1999b. Bio-optical properties of the marine diazotrophic cyanobacteria *Trichodesmium* spp. II. A reflectance model for remote sensing. *Limnol. Oceanogr.* 44(3):618–27

Subramaniam A, Carpenter EJ, Karentz D, Falkowski PG. 1999a. Bio-optical properties of the marine diazotrophic cyanobacteria *Trichodesmium* spp. I. Absorption and photosynthetic action spectra. *Limnol. Oceanogr.* 44(3):608–17

Sverdrup HU. 1953. On conditions for the veral blooming of phytoplankton. *J. Cons. Couseil Int. l'Exploration Mer* 18:287–95

Tjiputra JF, Polzin D, Winguth AME. 2007. Assimilation of seasonal chlorophyll and nutrient data into an adjoint three-dimensional ocean carbon cycle model: Sensitivity analysis and ecosystem parameter optimization. *Global Biogeochem. Cycles* 21:GB1001

Tomlinson MC, Stumpf RP, Ransibrahmanakul V, Truby EW, Kirkpatrick GJ, et al. 2004. Evaluation of the use of SeaWiFS imagery for detecting *Karenia brevis* harmful algal blooms in the eastern Gulf of Mexico. *Remote Sens. Environ.* 91:293–303

Uitz J, Claustre H, Morel A, Hooker SB. 2006. Vertical distribution of phytoplankton communities in open ocean: An assessment based on surface chlorophyll. *J. Geophys. Res.* 111:C08005

Uz BM, Yoder JA, Osychny V. 2001. Pumping of nutrients to ocean surface waters by the action of propagating planetary waves. *Nature* 409:597–600

Uz M, Yoder JA. 2004. High frequency and mesoscale variability in SeaWiFS chlorophyll imagery and its relation to other remotely sensed oceanographic variables. *Deep-Sea Res. II* 51:1001–17

Vance TC, Schumacher JD, Stabeno PJ, Baier CT, Wyllie-Echeverria T, et al. 1998. Aquamarine waters recorded for first time in eastern Bering Sea. *Eos. Trans. Am. Geophys. U.* 79(10):121

Wang M, Shi W. 2005. Estimation of ocean contribution at the MODIS near-infrared wavelengths along the east coast of the U.S.: Two case studies. *Geophys. Res. Lett.* 32:L13606

Werdell PJ, Bailey SW. 2005. An improved in-situ bio-optical data set for ocean color algorithm development and satellite data product validation. *Remote Sens. Environ.* 98:122–40

Westberry TK, Siegel DA, Subramaniam A. 2005. An improved bio-optical model for the remote sensing of *Trichodesmium* spp. blooms. *J. Geophys. Res.* 110:C06012

Westberry TK, Siegel DA. 2006. Spatial and temporal distribution of *Trichodesmium* blooms in the world's oceans. *Global Biogeochem. Cycles* 20:GB4016

Westberry TK, Behrenfeld MJ, Siegel DA, Boss E. 2008. Carbon-based primary productivity modeling with vertically resolved photoacclimation. *Global Biogeochem. Cycles* 22:GB2024

Wilson C, Adamec D. 2001. Correlations between surface chlorophyll and sea surface height in the tropical Pacific during the 1997–1998 El Niño-Southern Oscillation event. *J. Geophys. Res.* 106(C12):31175–88

Wilson C, Adamec D. 2002. A global view of bio-physical coupling from SeaWiFS and TOPEX satellite data, 1997–2001. *Geophys. Res. Lett.* 29(8):1257

Wilson C, Coles VJ. 2005. Global climatological relationships between satellite biological and physical observations and upper ocean properties. *J. Geophys. Res.* 110:C10001

Wynne TT, Stumpf RP, Tomlinson MC, Ransibrahmanakul V, Vallareal TA. 2005. Detecting *Karenia brevis* blooms and algal resuspension in the western Gulf of Mexico with satellite ocean color imagery. *Harmful Algae* 4:992–1003

Yoder JA, Kennelly MA. 2003. Seasonal and ENSO variability in global ocean phytoplankton chlorophyll derived from 4 years of SeaWiFS measurements. *Global Biogeochem. Cycles* 17(4):1112

Yoder JA, Kennelly MA. 2006. What have we learned about ocean variability from satellite ocean color imagers? *Oceanogr* 19(1):152–71

Zibordi G, Mélin F, Hooker SB, D'Alimonte D, Holben B. 2004. An autonomous above-water system for the validation of ocean color radiance data. *IEEE Trans. Geosci. Remote Sens.* 42(2):401–15

Zibordi G, Mélin F, Berthon J-F. 2006. Comparison of SeaWiFS, MODIS and MERIS radiometric products at a coastal site. *Geophys. Res. Lett.* 33:L06617

RELATED RESOURCES

Dickey T, Lewis M, Chang G, 2006. Optical oceanography: recent advances and future directions using global remote sensing and in situ observations. *Rev. Geophys*. 44:RG1001

Martin S. 2004. *An Introduction to Remote Sensing*. NY:Cambridge University Press. 454 pp.

McClain CR. Satellite remote sensing: ocean color, 2001. In *Encyclopedia of Ocean Sciences*, 1946–1959. London:Academic Press Ltd. (revised edition in press)

Siegel DA, Thomas AC, Marra J, eds. 2004. Special issue: Views of ocean processes from the Sea-viewing Wide Field-of-view Sensor (SeaWiFS) mission: Vol. 1. *Deep-Sea Res.* II 51:1–3

Siegel DA, Thomas AC, Marra J, eds. 2004. Special issue: Views of ocean processes from the Sea-viewing Wide Field-of-view Sensor (SeaWiFS) mission: Vol. 2. *Deep-Sea Res.* II 51:10–11
http://oceancolor.gsfc.nasa.gov/
http://web.science.oregonstate.edu/ocean.productivity/
http://www.ioccg.org

Annual Review of
Marine Science

Volume 1, 2009

Contents

Errata

An online log of corrections to *Annual Review of Marine Science* articles may be found at http://marine.annualreviews.org/errata.shtml